AIAA JOURNAL
Vol. 37, No. 6, June 1999

Coherent Anti-Stokes Raman Scattering Temperature Measurements on an Air-Breathing Ramjet Model

M. Fischer,* E. Magens,† H. Weisgerber,* A. Winandy,‡ and S. Cordes§
DLR, German Aerospace Research Center, 51170 Cologne, Germany

Coherent anti-Stokes Raman scattering was used to measure nitrogen single-pulse spectra at the entrance and exit area of a thrust nozzle. Thermodynamic nonequilibrium effects were proved at the exit of the hypersonic nozzle, belonging to an air-breathing, hydrogen-combusting ramjet model. To determine the accurracy of extracted rotational and vibrational temperatures, additional laboratory experiments were performed. The nozzle expansion was characterized by wall pressure measurements.

Introduction

THE presented investigations are a part of the Special Collaborative Research Program (SFB 253), a German basic research program in hypersonics, whose aim is the investigation of fundamental problems related to the design of aerospace planes. The research configuration is a two-stage space transport system similar to the Sänger configuration of the German National Hypersonic Technology Program, whose first stage has an air-breathing, hydrogen-fueled propulsion system (hybrid turbojet/ramjet). The design of future space transport systems must rely on computational fluid dynamics (CFD) codes because it is not possible to test all flight conditions experimentally. Of particular importance is the correct modeling of the flow in the propulsion system to get a precise prediction of the thrust. To verify and optimize flow simulation codes, model experiments are necessary, which analyze the properties of the flow in detail. In this study coherent anti-Stokes Raman scattering (CARS) temperature measurements are performed to analyze the thermodynamical behavior of the flow in a model thrust nozzle. Freezing of the vibrational temperature on a level higher than the translational temperature was expected due to the strong expansion in the propulsion system under study. The excess energy stored in internal molecular modes of motion is lost for the thrust of the propulsion system. This deviation from the thermal equilibrium would be obvious for a pure nitrogen expansion. But under the present conditions, the exhaust gas contains about 30% water. Therefore, the effective energy transfer of H_2O–N_2 collisions has to be taken into account for a simulation of the N_2 vibrational relaxation. The transition probability for H_2O–N_2 collisions is at least one to two orders of magnitude higher than for N_2–N_2 collisions.[1,2] Because differing data existed on the effectivity of such collisional processes, the quantitative examination of the relaxation process had to be supported by experimental data.

CARS was chosen for the temperature measurement because the exhaust gas mainly consists of nitrogen and water. Broadband CARS[3] enables nonintrusive single-pulse temperature measurements of these major gas constituents, which carry the main energy of the flow. Measured probability functions for the temperature allow an analysis of mixing processes in the combustion chamber (1–11 bar), as well as temperature measurements at the nozzle exit (60–115 mbar).

Because the spectral shape of CARS spectra is sensitive to both vibrational and rotational population, the rotational and vibrational temperatures can be extracted separately. This was the subject of several publications dealing with measurements on D_2 (Ref. 4), H_2 (Refs. 5 and 6), and N_2 (Refs. 7 and 8) in electric discharges and microwave excited N_2 (Ref. 9), N_2 near an incandescent filament,[10] and N_2 after the detonation of solid explosives.[11] Furthermore the CARS technique, adapted and used for temperature and concentration measurements since the 1970s (Refs. 12–14), was already successfully applied under the harsh conditions at ramjet facilities.[15–19] The application of CARS was reviewed in several publications; e.g., see Ref. 20, 21, or 22.

Experimental Setup

Test Facility

The thrust nozzle test facilities A and B at the German Aerospace Research Center (DLR), Cologne, have been presented previously.[23,24] Prior to this study, the temperature field at the exit of a combustion chamber in after burner technology was tested at the facility A.[25] Facility A was designed for nozzle development tests of short duration and had the capability of high mass flows up to 4 kg of air/s and 100 g of H_2/s at 10 bar. It was shown that the combustion was incomplete at the nozzle entrance. The smaller facility B was built for fundamental studies, which need longtime testing. Lower mass flow rates drastically reduce the costs, and the shorter optical path lengths facilitate the use of laser techniques in turbulent flames. The nozzle test facility B does not have the capability for thrust measurements but is especially designed for the use of optical measurement techniques. To simplify optical adjustments and to reduce measurement time, the test facility enables the movement and positioning of the object of investigation in all three space axes during operation. During the experiments, the position of the combustion chamber was automatically controlled and readjusted to compensate temperature-induced expansions. Figure 1 shows the object under examination. The facility was constructed according to the connected pipe principle. The combustion chamber is supplied with compressed air, which is preheated by two electrical heaters connected in parallel. After the reaction of hydrogen and air, the exhaust gas expands in the nozzle (Fig. 2). Optical access to the flow is provided at the entrance and exit of the nozzle by water-cooled adaptors to which window holders can be flanged. A wedge-shaped diffusor is used to reduce the pressure at the nozzle exit, which provides a capability of altitude simulation. At the top, the hot exhaust gas is cooled down by the injection of cold air and flows into a sound absorber.

The principle aim of the actual experiments was to provide experimental data for a comparison with numerical simulations. Therefore, the nozzle had to be supplied as homogeneously as possible with hot, pressurized exhaust gas. For this reason we used an in-house developed matrix-burner in the combustion chamber. This (microdiffusion) burner concept was successfully tested in previous laboratory experiments.[26] The big matrix burner used here (Fig. 3), consists of 127 closely packed tubes for the transport of preheated air. The hydrogen flows between these tubes. The air and hydrogen mass flows used are given in Table 1.

Presented as Paper 98-0961 at the AIAA 36th Aerospace Sciences Meeting, Reno, NV, Jan. 12–15, 1998; received Feb. 13, 1998; revision received June 15, 1998; accepted for publication June 25, 1998.

*Research Scientist, Institute of Propulsion Technology. Member AIAA.
†Research Scientist, Institute of Propulsion Technology; currently Chief, Software Development, RSB-Optotechnik GmbH, Quittenweg 48a, 90768 Fürth, Germany.
‡Technician, Institute of Propulsion Technology.
§Engineer, Institute of Propulsion Technology.

Table 1 Mass flows and air temperatures used in the experiments

Pressure	1 bar	11 bar
Air temperature, K	600	900
H_2 mass flow, g/s	2	8.8
Air mass flow, g/s	70	300

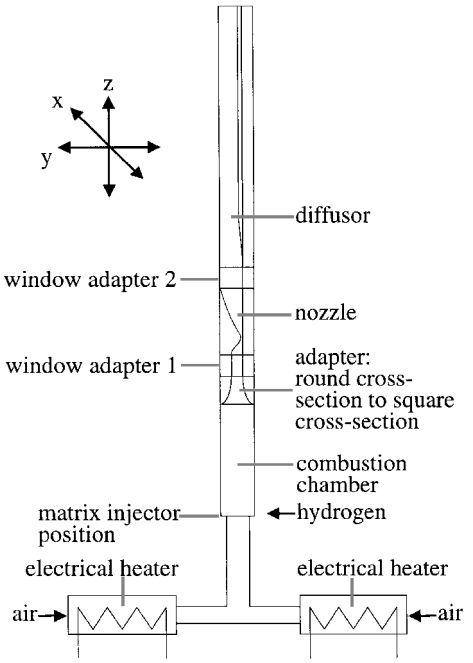

Fig. 1 Thrust nozzle test facility B; gas flow direction is from the bottom to the top.

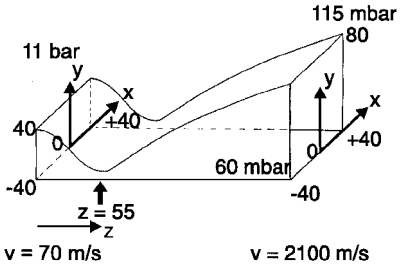

Fig. 2 Nozzle geometry and coordinate system corresponding to the results: optical axis for the measurements parallel to the x axis; x, y, and z dimensions given in millimeters; pressures and flow velocities at the entrance and exit area of the nozzle are given.

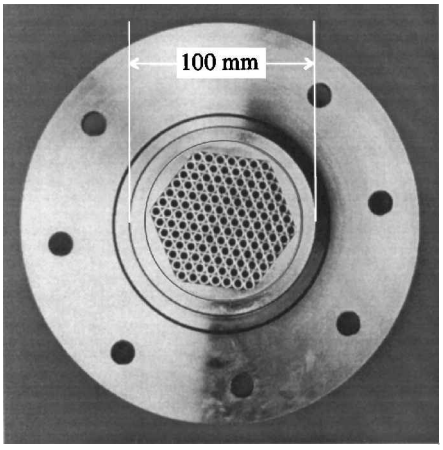

Fig. 3 Matrix injector for hydrogen and air; inner diameter of the combustion chamber, 100 mm.

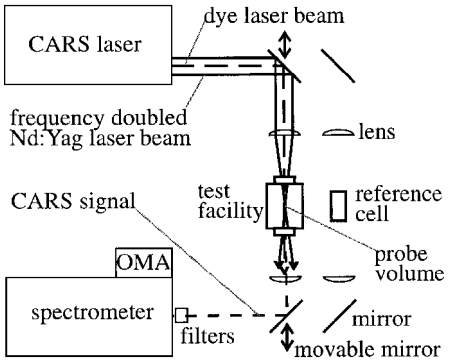

Fig. 4 CARS setup: view from the top for the folded BOXCARS arrangement.

CARS System and Experimental Background

A commercial broadband CARS system, SOPRA, was used, which is optimized for flame measurements. Figure 4 shows the CARS setup, which mainly consists of two stable units. The first contains the CARS laser and the second the spectrometer and the detector. Spectrometer and laser were located inside of the test facility during the experiments and controlled from a neighboring room separated by concrete walls. The data evaluation and part of the data acquisition were developed at the DLR, Cologne, and especially adapted for measurements at high temperature and pressure.[26,27] The CARS system was successfully applied in several applications, e.g., Refs. 28 and 29. The laser system is based on a frequency-stabilized, injection-seeded, single-mode Nd:Yag laser. The stable infrared resonator emits pulsed radiation with a near Gaussian intensity beam profile at a wavelength of 1064 nm. This laser beam is first amplified and then frequency doubled in a KDP-crystal resulting in the pump beam (ν_1) with a wavelength of 532 nm. The pump beam has a pulse length of 14 ns, a repetition rate of 10 Hz, and a pulse energy of 42 mJ at the laser exit. To generate the Stokes beam, rhodamin 610 was used in the oscillator and amplifier cell of the dye laser. The dye laser is pumped transversely by a portion of the green laser beam and emits broadband radiation (ν_2) with a pulse energy of about 3.5 mJ. The polarization of pump and Stokes beam were parallel, relative to each other.

Because of the broadband operation of the dye laser, with each laser pulse it is possible to record a complete nitrogen CARS spectrum, which can be evaluated giving a single-pulse temperature. For the evaluation of the signals, the spectral intensity distribution of the dye laser is taken into account by normalization with a reference spectrum measured in argon. The typical spectral width of the reference spectrum amounts to 110 cm^{-1} full width at half-maximum. The frequency stability of the dye laser was verified by recording reference spectra prior to and after the measurements. The variation of the mean temperature caused by residual small frequency drifts of the dye laser was less than 1%. For the temperature range of these measurements, the data evaluation could be limited to Raman shifts ($\nu_{RS} = \nu_1 - \nu_2$) between 2276 and 2345 cm^{-1}. This spectral range covers the Q-branch transitions originating from the first two vibrational states of nitrogen and is also shown in the mean CARS spectrum of Fig. 5.

The experiments at the nozzle entrance were performed in a planar BOXCARS beam arrangement and at the nozzle exit in a folded BOXCARS beam arrangement.[30] The probe volume is formed by three crossing laser beams, which interact with the medium and generate a signal beam at $\nu_{CARS} = \nu_1 + \nu_{RS}$. An achromatic lens with a focal length of 300 mm was used to focus the laser beams. The corresponding probe volume, in which 95% of the CARS signal is generated, had a length of 3.2 mm under laboratory conditions. The absence of stimulated Raman effects, which can result in an excess vibrational population, was proved by measurements in a low-pressure cell. As a consequence of the high CARS efficiency reached with the single-mode laser system, even at the highest available laser powers we never found a population distortion due to such effects.

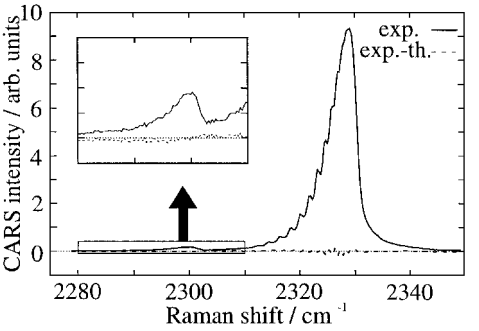

Fig. 5 Mean N_2-CARS spectrum belonging to the ensemble in Fig. 13, measured at the nozzle exit; nonequilibrium population of the vibrational states is demonstrated by the two-dimensional temperature fit to ground-state fundamental band ($v = 0 \rightarrow 1$) and first hotband ($v = 1 \rightarrow 2$): $T_{rot} = 831$ K and $T_{vib} = 1124$ K.

The optical axis for the measurements was adjusted parallel to the x axis, shown in Fig. 2. The signals were guided by mirrors, coupled into the spectrometer, and finally imaged on the detector by a concave reflection grating (Jobin Yvon, 2100 lines/mm). A linear photodiode array with 512 diodes (model 1420/HQ from EG&G) was used as detector. The phosphorus P46 of the image intensifier has a decay time in the nanosecond range.

The temperatures were evaluated by a weighted fit of the measured single-pulse spectra to precalculated theoretical spectra, stored in a spectra library. The CARS theory has been described, e.g., in Refs. 21 and 31–33. We used a home-made code,[34] which calculates the third-order, nonlinear susceptibility according to an expression given in Ref. 35 and strategies given in Refs. 21 and 36, including Doppler and collisional broadening. The collisional broadening portions of the line broadening, compare Eqs. (11) and (15) in Ref. 37, were determined based on the use of the energy corrected sudden exponential power (ECS-EP) law[38] for the N_2–H_2O relaxation rates and by a modified (m)-ECS-EP law[26] for the N_2–N_2 relaxation rates. The m-ECS-EP uses an amplitude factor $A(T)$ similar to the factor given in Ref. 39. Different fitting and scaling laws were tested in the high-temperature range.[26] In laboratory studies on a hydrogen/air-fueled burner at about 10 bar, 2360 K, we yielded comparable results using a combination of modified exponential-gap high temperature (MEG-HT)[40] for the nitrogen self-broadening and MEG[37] for the N_2–H_2O relaxation rates. A detailed discussion of the influence of these laws[37–41] is clearly outside of the scope of this work and will be published shortly.

For the evaluation of independent rotational and vibrational temperatures, a two-dimensional library was used. The fit was based on the assumption of independent Boltzmann distributions for the rotational and vibrational populations. This should be valid according to an estimation made by the use of Ref. 42.

In the weighting process, the average intensity profile of the dye laser, CARS specific noise, and detector properties are accounted for. As main criterion in the selection of pertubed spectra, e.g., due to breakdown in the gas caused by particles in the laser focus, the intensity independent relative deviation of the experimental to the fitted theoretical spectra was used.

Typically, a sequence of 1200 single-shot broadband spectra was recorded for one ensemble at a given measurement position. The total integral intensity of the single-pulse spectra measured at low pressure was clearly above the lower limit. The good spectral resolution reached in the experiments at low pressure (Fig. 5) and under atmospheric conditions is advantageous for the determination of the rotational temperature and makes the identification of mixed temperature spectra easier.

The root mean square value of the one-dimensional single-pulse temperatures and the absolute accuracy of the mean values are known from experiments under laboratory conditions at temperatures up to 3000 K and pressures up to 10 bar (Refs. 26 and 27). At, e.g., 1600 K, the root mean square value of the single-pulse temperatures is less than 40 K (Ref. 27). The accuracy of the mean temperatures is, under the given experimental conditions at the test facility, about 2–3% for a one-dimensional temperature fit and 4% for the independent fit of T_{rot} and T_{vib}.

Results and Discussion

To obtain information on the stability of our two-dimensional library fit, we performed experiments in an oven cell. For a set of different constant temperatures, we varied the signal level (Fig. 6). The root mean square values of the one-dimensional temperature fit and simultaneous fit of T_{rot} and T_{vib} are compared in Fig. 6. Depending on the signal intensity in the first hotband, the reproducibility of the single-pulse vibrational temperatures decreases drastically at low temperatures. For the vibrational temperature range found at the nozzle exit, rms(T_{vib}) increases stronger than rms(T_{rot}) at low signal intensities. The graphite furnace used (HGA 500 from Perkin Elmer) was the same as described in Ref. 27. Although the oven experiments were done at atmospheric conditions, a good estimation of the possible errors at low pressure can be given from the results at the same signal to noise ratio and 1 atm.

The temperature homogeneity of the flowfield at the entrance area of the nozzle has been verified under atmospheric conditions. Figure 7 shows the achieved boxlike, equalized temperature profile, which is flat within about ±35 K. This is more obvious in the centerline plot, Fig. 8, where additionally the width of temperature probability density functions (PDFs) is given. The narrow PDFs correspond to a typical rms (T) value of 52 K in the center area. Taking into consideration the preheated air (600 K) we found a difference of 270 K to a calculated equilibrium temperature. This difference is caused by a combination of three factors. First, an estimated heat loss of about 100 K. Second, incomplete energy conversion of the reaction resulting in a 140 K lower temperature, and finally, the transition time in the combustion chamber of about 0.006 s, which is slightly insufficient to reach equilibrium conditions. Subsequent concentration measurements of samples taken with a suction gas probe yielded an energy conversion of 93.5% and a nearly constant water content of about 30% of the exhaust gas.[43]

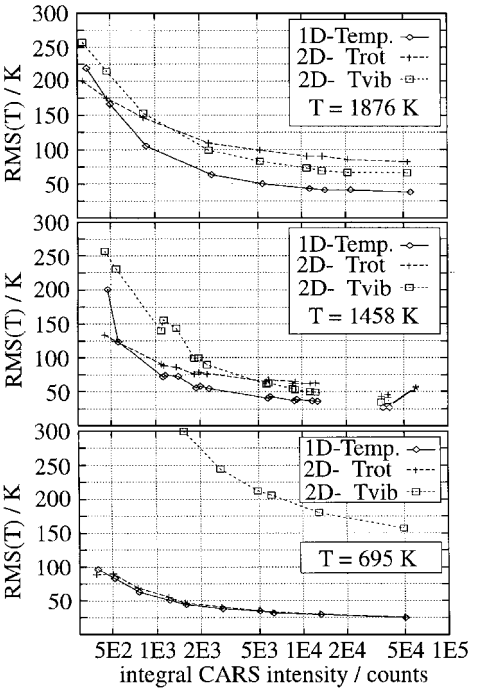

Fig. 6 Furnace experiments at 1 atm; ∗, measured at 1254 K.

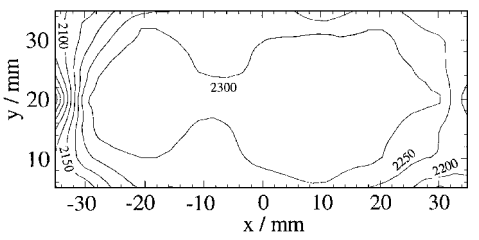

Fig. 7 Temperature distribution at the nozzle entrance measured under atmospheric conditions; temperature of the preheated air, 600 K.

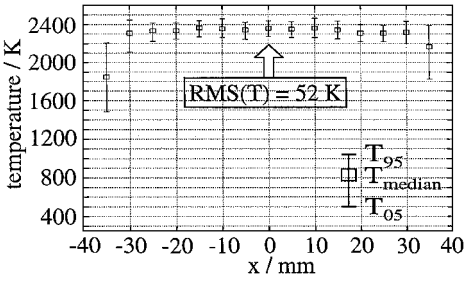

Fig. 8 Temperature profile at $y = 20$ mm shows narrow temperature PDFs, a typical value for rms (T) is given; 5% of the temperatures are lower than T_{05}, and 5% of the temperatures are higher than T_{95}.

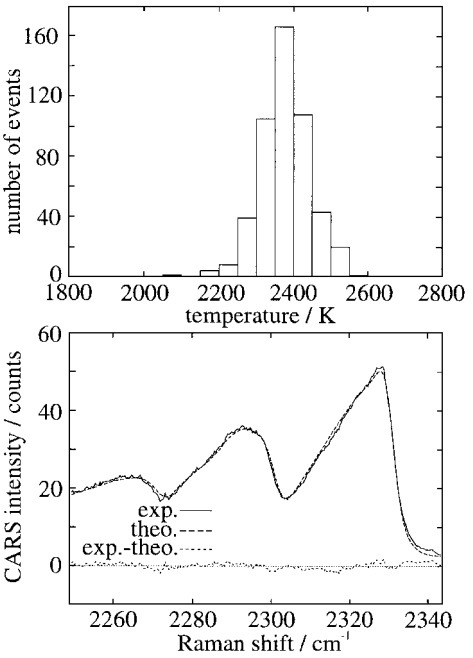

Fig. 9 Temperature PDF and mean N_2-CARS spectrum measured at the nozzle entrance; mean spectrum taken averaging all valid single-pulse spectra from the maximum of the distribution; combustion chamber pressure, 11 bar; and temperature of the preheated air, 900 K.

At 11-bar combustion chamber pressure, the CARS signal intensity was reduced by diffraction index fluctuations, which caused vehement laser beam distortions. Nevertheless, measurements in the center of the nozzle entrance area were possible at the expense of increased measurement time. The result is shown in Fig. 9. A narrow temperature PDF was found at a median temperature of 2375 K. Previously performed laboratory experiments on a smaller high-pressure matrix burner proved a flat temperature profile. In view of the costs for the actual experiment and because of expected Reynolds invariance of the flow, we have not performed further measurements in the high-pressure zone up to now. We first continued with experiments at the nozzle exit.

The measurement areas at the entrance and exit of the nozzle are indicated in Fig. 2. Laser-two-focus velocimetry measurements yielded a velocity of 70 m/s at the nozzle entrance and about 2100 m/s at the exit with an equalized velocity profile along the x axis.[44] The temperature measurements at the nozzle exit (Figs. 10 and 11) showed a marked difference between rotational (equal to translational) and vibrational temperature of the nitrogen molecule. Along the y axis, the rotational temperature T_{rot} increases nearly linearly from 600 K near the plane wall (60 mbar) to 860 K at the contoured wall (115 mbar). The stronger expansion on the plane side does not only result in a lower rotational temperature but also in an earlier freezing of the vibrational relaxation and, therefore, in an increased nonequilibrium. The variation of the vibrational temperature (T_{vib}) is smaller. T_{vib} rises to a maximum of about 1190 K at $y = 40$ mm with a subsequent slight decrease. A smaller nonequilibrium is found at the contoured wall of the nozzle. Along the x axis, a

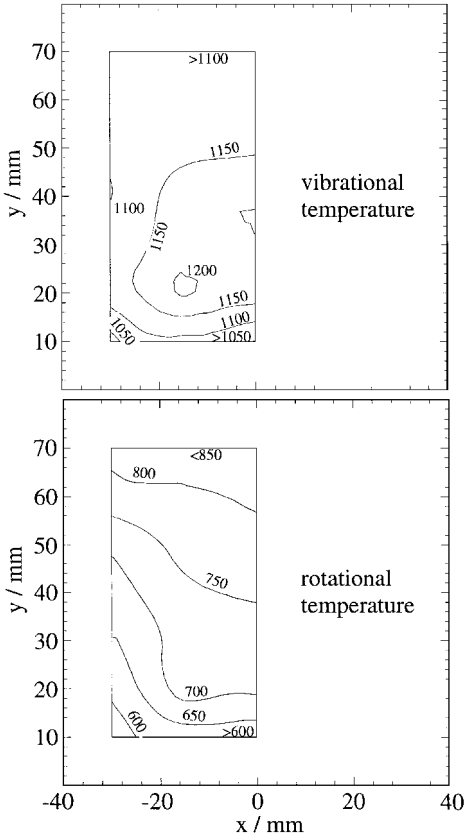

Fig. 10 Measured distributions of T_{rot} and T_{vib} at the nozzle exit visualizing the thermal nonequilibrium.

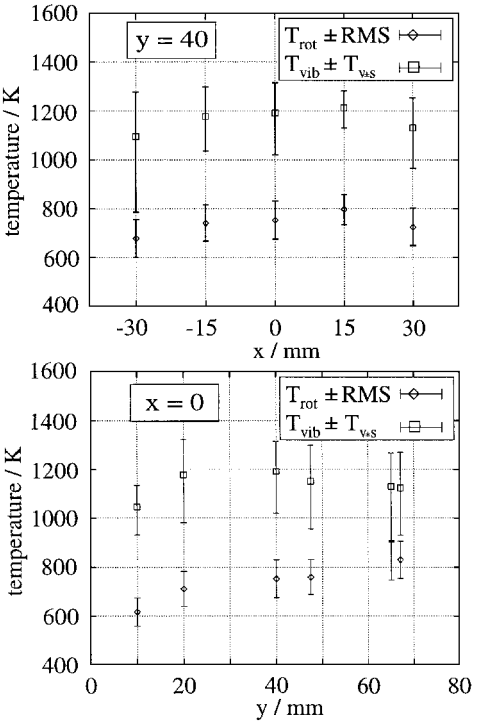

Fig. 11 Temperature profiles along x axis (top) and y axis (bottom) at the nozzle exit.

nearly symmetric profile was found for T_{rot} and T_{vib}, with a plateau in the middle of the flow. The relatively small thermal nonequilibrium of the nitrogen (about 400 K) is due to the high water content of the flow. The more efficient energy transfer of collisions with water causes an improved relaxation of the nitrogen and a freezing of the vibrational relaxation farther downstream.

In Figs. 12 and 13, the PDFs for T_{rot} and T_{vib} are given at two positions. The small asymmetry and scatter toward the lower

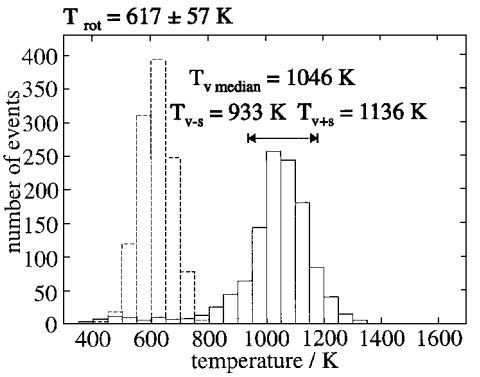

Fig. 12 Temperature PDF measured at the nozzle exit ($x = 0$ mm, $y = 10$ mm) near to the plane wall: 15.9% of the single-pulse temperatures are lower than T_{v-s} and 15.9% of the single-pulse temperatures are higher than T_{v+s}.

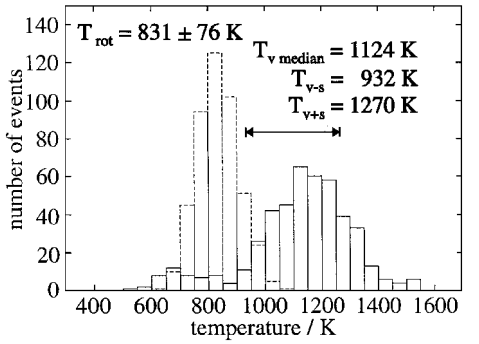

Fig. 13 Temperature PDF measured at the nozzle exit ($x = 0$ mm, $y = 67$ mm) near to the contoured side: 15.9% of the single-pulse temperatures are lower than T_{v-s} and 15.9% of the single-pulse temperatures are higher than T_{v+s}.

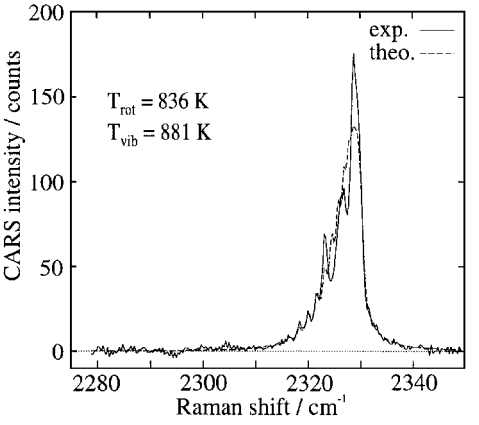

Fig. 14 Single-shot spectrum at low vibrational temperature showing no thermal nonequilibrium.

temperatures seen in the T_{vib} data are also a consequence of the vanishing temperature sensitivity when no hotband can be monitored. This is illustrated by the single-shot spectrum shown in Fig. 14. But the mean nonequilibrium could be clearly measured under the given conditions. The accuracy of T_{vib} is still about an order of magnitude better than the temperature difference to be measured. Additionally, the part of the rms (T) produced by CARS itself was about 38 K for T_{rot} and 100 K for T_{vib}, known from the oven measurements evaluated at the signal to noise ratio of the nozzle experiment. Both values are clearly smaller than the measured PDF widths. Nevertheless, a considerable number of events clearly shows no excess vibrational population. Hence, the vibrational temperature PDF of the nozzle flowfield cannot be Gaussian.

Figure 5 shows a mean nitrogen spectrum at the nozzle exit belonging to the single-pulse data ensemble in Fig. 13. For the

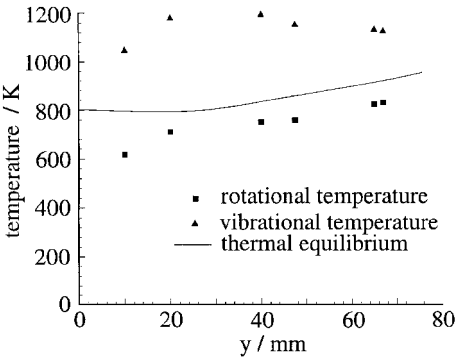

Fig. 15 Comparison of CARS temperatures and temperature results of an Euler calculation.

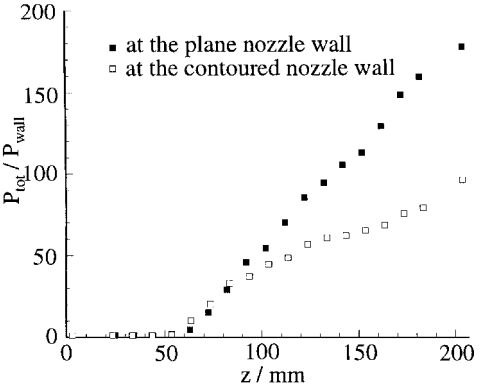

Fig. 16 Experimental wall pressure data given as ratio total pressure to wall pressure.

ground state fundamental band ($v = 0 \rightarrow 1$) and the first hotband ($v = 1 \rightarrow 2$), a good agreement of theory and experiment is found with the same set of (T_{rot}, T_{vib}). A comparison of the measured temperature data in y direction (Fig. 11 bottom) with a calculation by a two-dimensional finite element code solving the Euler equations for a chemically reacting mixture of ideal gases[45,46] using a reduced chemical kinetics scheme[47] is shown in Fig. 15. The Euler calculation based on experimentally determined nozzle entrance conditions (2375 K and 70 m/s), assumed chemical equilibrium species concentrations at the nozzle entrance and homogeneous concentration profiles. It matches the slope of the experimental rotational temperatures fairly well for $y \geq 20$ mm. But the rotational temperatures calculated are about 100 K higher. To explain the discrepancies more sophisticated Navier–Stokes calculations are in preparation to include the boundary layer, which reduces the effective free area of the flow, the expansion ratio, and the velocity. Additionally, freezing of the vibrational energy has to be taken into account. The amount of vibrational energy stored in the molecules is lost for the expansion, resulting in lower velocities and translational temperatures ($=T_{rot}$) at the nozzle exit.

Wall Pressure Measurements

The measured wall pressure data (Fig. 16) reflect the development of the expansion. To recall the z axis and shape of the nozzle, compare Fig. 2. The expansion ratio A/A^* is 12.5 for the nozzle. The flow accelerates more strongly on the contoured side near the nozzle throat. This behavior is in good agreement with Euler calculations[45] shown in Fig. 17. Farther downstream, the expansion on the plane side is much stronger and reduces the wall pressure to 60 mbar at the exit, compared to 115 mbar at the contoured wall.

Conclusion

A matrix burner has been developed and was successfully used to generate an equalized temperature field at the entrance of a hypersonic nozzle. Single-pulse N_2-CARS temperature measurements with high spatial and temporal resolution were performed to characterize the flowfield in entrance and exit area of the nozzle.

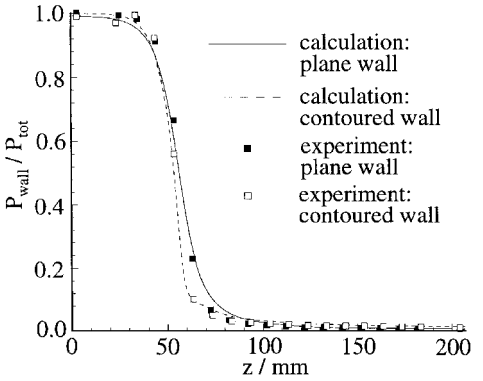

Fig. 17 Experimental nozzle wall pressure data compared to pressure results of an Euler calculation.

The flow shows a marked chemical and thermal nonequilibrium because molecular exchange processes cannot keep the pace of the expansion. Previous numerical calculations verified the freezing of chemical reactions near the nozzle throat. The complete description of the expansion requires an included simulation of the vibrational energy content. The measured data will serve as a basis for the optimization of flow calculations, including the influence of N_2–H_2O collisions on the nitrogen relaxation.

Acknowledgments

This work was financially supported by the Deutsche Forschungsgemeinschaft (SFB 253, No. C8). The authors gratefully acknowledge the technical support of M. Graben and W. Seelig. We thank T. Link for the permission to present his calculations. The coherent anti-Stokes Raman scattering (CARS) team at the DLR, German Aerospace Research Center, Cologne, especially acknowledges numerous helpful discussions in the past with Marc Bucchia (SOPRA), as well as Michel Péalat and his group at ONERA.

References

[1]Cottrell, T. L., and McCoubrey, J. C., *Molecular Energy Transfer in Gases*, Butterworths, London, 1961, pp. 78–97.

[2]Taylor, R. L., and Bitterman, S., "Survey of Vibrational Relaxation Data for Processes Important in the CO_2–N_2 Laser System," *Reviews of Modern Physics*, Vol. 41, No. 1, 1969, pp. 26–47.

[3]Roh, W. B., Schreiber, P. W., and Taran, J. P., "Single-Pulse Coherent Anti-Stokes Raman Scattering," *Applied Physics Letters*, Vol. 29, No. 3, 1976, pp. 174–176.

[4]Nibler, J. W., McDonald, J. R., and Harvey, A. B., "CARS Measurements of Vibrational Temperatures in Electric Discharges," *Optics Communications*, Vol. 18, No. 3, 1976, pp. 371–373.

[5]Péalat, M., Taran, J. P., Taillet, Y., Bacal, M., and Bruneteau, A. M., "Measurement of Vibrational Populations in Low-Pressure Hydrogen Plasma by Coherent Anti-Stokes Raman Scattering," *Journal of Applied Physics*, Vol. 52, No. 4, 1981, pp. 2687–2691.

[6]Bornemann, T., Kornas, V., Schulz-von der Gathen, V., and Döbele, H. F., "Temperature and Concentration Measurements of Molecular Hydrogen in a Filamentary Discharge by Coherent Anti-Stokes Raman Spectroscopy (CARS)," *Applied Physics B*, Vol. 51, 1990, pp. 307–313.

[7]Shaub, W. M., Nibler, J. W., and Harvey, A. B., "Direct Determination of Non-Boltzmann Vibrational Level Populations in Electric Discharges by CARS," *Journal of Chemical Physics*, Vol. 67, No. 5, 1977, pp. 1883–1886.

[8]Massabieaux, B., Gousset, G., Lefebvre, M., and Péalat, M., "Determination of $N_2(X)$ Vibrational Level Populations and Rotational Temperatures Using CARS in a D.C. Low Pressure Discharge," *Journal de Physique*, Vol. 48, Nov. 1987, pp. 1939–1949.

[9]Dreier, T., Wellhausen, U., and Wolfrum, J., "CARS Studies of Vibrationally Excited Nitrogen at Low Pressures," *Applied Physics B*, Vol. 29, 1982, pp. 31–36.

[10]Dring, I. S., Devonshire, R., Meads, J., Boysan, H. F., and Greenhalgh, D. A., "Observation of Non-Equilibrium Effects in Free-Convective Flows Using CARS. Recirculating Flow Relaxation Spectrometry," *Chemical Physics Letters*, Vol. 132, No. 3, 1986, pp. 283–290.

[11]Grish, F., Péalat, M., Bouchardy, P., and Taran, J. P., "Real Time Diagnostics of Detonation Products from Lead Azide Using Coherent Anti-Stokes Raman Scattering," *Applied Physics Letters*, Vol. 59, No. 27, 1991, pp. 3516–3518.

[12]Régnier, P. R., and Taran, J. P. E., "On the Possibility of Measuring Gas Concentrations by Stimulated Anti-Stokes Scattering," *Applied Physics Letters*, Vol. 23, No. 5, 1973, pp. 240–242.

[13]Moya, F., Druet, S. A. J., and Taran, J. P. E., "Gas Spectroscopy and Temperature Measurement by Coherent Raman Anti-Stokes Scattering," *Optics Communications*, Vol. 13, No. 2, 1975, pp. 169–174.

[14]Hall, R. J., "CARS Spectra of Combustion Gases," *Combustion and Flame*, Vol. 35, 1979, pp. 47–60.

[15]Eckbreth, A. C., Anderson, T. J., and Dobbs, G. M., "Multi-Color CARS for Hydrogen-Fueled Scramjet Applications," *Applied Physics B*, Vol. 45, 1988, pp. 215–223.

[16]Anderson, T. J., and Eckbreth, A. C., "Simultaneous Measurements of Temperature and H_2, H_2O Concentrations in Hydrogen-Fueled Supersonic Combustion," AIAA Paper 90-0158, Jan. 1990.

[17]Jarrett, O., Jr., Antcliff, R. R., Smith, M. W., Cutler, A. D., Diskin, G. S., and Northam, G. B., "CARS Temperature Measurements in Turbulent and Supersonic Facilities," *7th International Symposium on Temperature: Its Measurement and Control in Science and Industry*, edited by J. F. Schooley, American Inst. of Physics, New York, 1992, pp. 667–672.

[18]Smith, M. W., Jarrett, O., Jr., Antcliff, R. R., Northam, G. B., Cutler, A. D., and Taylor, D. J., "Coherent Anti-Stokes Raman Spectroscopy Temperature Measurements in a Hydrogen-Fueled Supersonic Combustor," *Journal of Propulsion and Power*, Vol. 9, No. 2, 1993, pp. 163–168.

[19]Waidmann, W., Alff, F., Böhm, M., Clauß, W., and Oschwald, M., "Supersonic Combustion of Hydrogen/Air in a Scramjet Combustion Chamber," *Space Technology*, Vol. 15, No. 6, 1995, pp. 421–429.

[20]Hall, R. J., and Eckbreth, A. C., "Coherent Anti-Stokes Raman Spectroscopy (CARS): Application to Combustion Diagnostics," United Technologies Research Center, East Hartford, CT, July 1981; also *Laser Applications*, Vol. 5, edited by J. F. Ready and R. K. Erf, Academic, Orlando, FL, 1984, pp. 213–309.

[21]Greenhalgh, D. A., "Quantitative CARS Spectroscopy," *Advances in Non-Linear Spectroscopy*, edited by R. J. H. Clarke and R. E. Hester, Wiley, New York, 1987, Chap. 5.

[22]Eckbreth, A. C., *Laser Diagnostics for Combustion Temperature and Species*, Abacus, Cambridge, MA, 1988, Chaps. 4 and 6.

[23]Hungenberg, H., Stursberg, K., and Weyer, H., "Thrust Nozzle Test Facility at DLR Cologne," AIAA Paper 91-5024, Dec. 1991.

[24]Stursberg, K., and Hungenberg, H., "Errichtung eines Düsenprüfstandes für Hochtemperaturuntersuchungen an Schubdüsen von Hyperschallantrieben," DLR, German Aerospace Research Establishment, DLR-Internal Rept. IB 325-02-93, Cologne, Germany, Jan. 1993.

[25]Fischer, M., Magens, E., and Winandy, A., "N_2- und H_2O-CARS-Einzelpulsmessungen in planarer BOX-CARS-Konfiguration an der mit H_2 und Luft betriebenen Brennkammer des BDP-A," DLR, German Aerospace Research Establishment, DLR-Internal Rept. IB-325-12-94, Cologne, Germany, Feb. 1994.

[26]Fischer, M., Magens, E., and Winandy, A., "N_2 and H_2O Thermometry at High Pressure and Temperature," XIV European CARS Workshop, Poster B-7, March 1995.

[27]Fischer, M., Magens, E., and Winandy, A., "Single-Shot Broadband Nitrogen CARS Measurements with Temperatures up to 3200 K: Comparison of Different Data Evaluation Schemes," *Coherent Raman Spectroscopy: Applications and New Developments*, World Scientific, Singapore, 1993, pp. 165–170.

[28]Koopman, J., Fischer, M., Magens, E., Winandy, A., and Meislitzer, B., "Potential Use of Hydrogen in Propulsion," DLR, German Aerospace Research Establishment, European Community Rept., EC Contract 5077-92-11 EL ISP D, EQHHPP Phase III.0-3, Subtask: Non-Intrusive Measurements, Inst. of Propulsion Technology, Cologne, Germany, Jan. 1996.

[29]Griebel, P., Fischer, M., Hassa, C., Magens, E., Nannen, H., Winandy, A., Chrisostomou, A., Meier, U., and Stricker, W., "Experimental Investigation of an Atmospheric Rectangular Rich Quench Lean Combustor Sector for Aeroengines," American Society of Mechanical Engineers, ASME 97-GT-146, Orlando, FL, June 1997.

[30]Eckbreth, A. C., "BOXCARS: Crossed-Beam Phase-Matched CARS Generation in Gases," *Applied Physics Letters*, Vol. 32, No. 7, 1978, pp. 421–423.

[31]Nibler, J. W., and Knighten, G. V., "Coherent Anti-Stokes Raman Spectroscopy," *Topics in Current Physics 11: Raman Spectroscopy of Gases and Liquids*, edited by A. Weber, Springer, 1979, pp. 253–299.

[32]Druet, S. A., and Taran, J. P., *Progress in Quantum Electronics*, Vol. 7, Pergamon, Oxford, England, UK, 1981, pp. 1–72.

[33]Levenson, M. D., and Kano, S. S., *Introduction to Nonlinear Laser Spectroscopy*, rev. ed., Academic, New York, 1988, Chap. 4.

[34]Magens, E., "CARS-Code of the Institute of Propulsion Technology," DLR, German Aerospace Research Establishment, Cologne, Germany, 1996.

[35]Hall, R. J., Verdieck, J. F., and Eckbreth, A. C., "Pressure-Induced Narrowing of the CARS Spectrum of N_2," *Optics Communications*, Vol. 35, No.1, 1980, pp. 69–75.

[36]Koszykowski, M. L., Farrow, R. L., and Palmer, R. E., "Calculation of Collisionally Narrowed Coherent Anti-Stokes Raman Spectroscopy Spectra," *Optics Letters*, Vol. 10, No. 10, 1985, pp. 478–480.

[37]Bonamy, J., Robert, D., Hartmann, J. M., Gonze, M. L., Saint-Loup, R., and Berger, H., "Line Broadening, Line Shifting, and Line Coupling Effects on N_2–H_2O Stimulated Raman Spectra," *Journal of Chemical Physics*, Vol. 91, No. 10, 1989, pp. 5916–5925.

[38]Millot, G., "Rotationally Inelastic Rates over a Wide Temperature Range Based on an Energy Corrected Sudden-Exponential-Power Theoretical Analysis of Raman Line Broadening Coefficients and Q-Branch Collapse," *Journal of Chemical Physics*, Vol. 93, No. 11, 1990, pp. 8001–8010.

[39]Farrow, R. L., Trebino, R., and Palmer, R. E., "High-Resolution CARS Measurements of Temperature Profiles and Pressure in a Tungsten Lamp," *Applied Optics*, Vol. 26, No. 2, 1987, pp. 331–335.

[40]Lavorel, B., Guillot, L., Bonamy, J., and Robert, D., "Collisional Raman Linewidth of Nitrogen at High Temperature (1700–2400 K)," *Optics Letters*, Vol. 20, No. 10, 1995, pp. 1189–1191.

[41]Rahn, L. A., and Palmer, R. E., "Studies of Nitrogen Self-Broadening at High Temperature with Inverse Raman Spectroscopy," *Journal of the Optical Society of America B*, Vol. 3, No. 9, 1986, pp. 1164–1169.

[42]Center, R. E., and Caledonia, G. E., "Anharmonic Effects on the Rate of Relaxation of Vibrational Energy in Rapidly Expanding Flows," *Journal of Chemical Physics*, Vol. 57, No. 9, 1972, pp. 3763–3770.

[43]Ciezki, H. K., and Brändle, R., "Bestimmung der Speziesverteilungen im Eintrittsquerschnitt zur Experimentalkammer am Brennkammer-Düsen-Prüfstand BDP-B," DLR, German Aerospace Research Establishment, DLR-Internal Rept. IB 645-97-06, Cologne, Germany, Feb. 1997.

[44]Weisgerber, H., Fischer, M., Magens, E., Winandy, A., Beversdorff, M., Förster, W., Cordes, S., and Meislitzer, B., "Experimentelle Untersuchungen zur Expansionsströmung nach Wasserstoff/Luft-Verbrennung in luftatmenden Hyperschallantrieben," DLR, German Aerospace Research Establishment, DLR-Internal Rept. IB-325-04-97, Cologne, Germany, April 1997.

[45]Link, T., Fox, U., and Koschel, W., "Computation of High Speed Reacting Flows Using a Finite Element Method," Tagung der Gesellschaft für Angewandte Mathematik und Mechanik (GAMM), Regensburg, Germany, March 1997.

[46]Fox, U., Rick, W., and Koschel, W., "Computation of Hypersonic High Temperature Nozzle Flow," *Zeitschrift für Flugwissenschaften und Weltraumforschung*, Vol. 17, No. 2, 1993, pp. 139–148.

[47]Mühleck, P., "Numerische Untersuchungen turbulenter, reagierender Strömungen in Brennkammern und Schubdüsen von Hyperschall-Staustrahltriebwerken," Ph.D. Thesis, Fakultät für Maschinenbau, Ruhr-Univ. Bochum, Germany, June 1995; also DLR-Rept. 95-18, DLR, German Aerospace Research Establishment, Cologne, Germany, June 1995.

R. P. Lucht
Associate Editor